Analysis of the Laser Beam Trajectory and its Impact on the Cut in PMMA Material

Journal of Physics: Conference Series **3157** (2025) 012027 doi:10.1088/1742-6596/3157/1/012027

Analysis of the Laser Beam Trajectory and its Impact on the Cut in PMMA Material

J Knedlová*, O Bílek and D Bartík

Tomas Bata University in Zlín, Department of Production Engineering, Vavrečkova 5669, 760 01 Zlín, Czechia

*E-mail: knedlova@utb.cz

Abstract. Article investigates how laser toolpath interpolation (linear vs. circular) affects kerf width, dimensional accuracy, and kerf taper when CO_2-cutting PMMA sheets (t = 3, 5 mm) on an ILS 3NM system (λ = 10.6 μm; P = 100 W). Lenses with f = 1.5" and 2.5″ were assessed. At identical process settings adopted from prior work, linear toolpaths yielded larger outer dimensions and more pronounced kerf taper, whereas circular paths produced more stable kerf and smaller taper angles. In all cases, the top-surface kerf exceeded the bottom-surface kerf. Thinner sheets (3 mm) were more sensitive to focal length and heat accumulation. The results provide practical guidance for selecting optics and toolpaths to balance accuracy and edge quality in PMMA cutting and form an experimental basis for future AI-assisted process optimization.

1. Introduction

In recent years, laser cutting has become a key technology in modern manufacturing due to its high precision, efficiency, and versatility. As this field continues to advance, new trends are emerging that are fundamentally changing the way laser cutting is implemented in various industries.

One of the main trends is automation. Modern laser cutting systems are becoming more autonomous, enabling faster, more efficient production with minimal human intervention. Fully automated systems can control entire production lines, which is particularly beneficial in the automotive and aerospace industries. [1-4]

Another significant trend is the integration of artificial intelligence (AI). AI-based algorithms enable laser cutting machines to achieve greater precision and adaptability, improving cutting quality and efficiency overall. [5-6]

The growing emphasis on sustainability is leading to the development of more environmentally friendly laser cutting technologies. Modern laser systems are designed to be more energy-efficient, thereby reducing operating costs and environmental impact. Other key aspects of a sustainable production process include optimizing the use of materials and reducing waste. Improved material capabilities allow laser cutting machines to process a wider range of materials, including metals, plastics, and composites. This expands their use in various industries, such as healthcare and electronics.

Integrating laser cutting with digital technologies and Industry 4.0 allows for more effective monitoring and control of production processes. The use of sensors and data analytics to optimize performance and quality is becoming increasingly common. [7-8]

The growing demand for customized and personalized products is leading to the development of laser cutting technologies that allow for quick and precise adjustments to designs based on specific customer requirements.

To take full advantage of AI, it is essential to specify the data that AI can correctly process. This data could include experimentally verified working conditions for laser equipment. [9-10]

Optimizing laser device settings for different materials involves several key steps and parameters, such as cutting speed, laser power, material-specific focal length, and the thickness of the material to be machined. Since each material has its own specific requirements, it is important to experiment and modify based on specific conditions and requirements regarding cutting width, surface finish, cutting angle, and HAZ. [11-13]

Significant experiments on laser cutting metals, composites, and alloys are already available. However, breakthroughs have also been made in laser cutting polymer materials in the last few decades. Nevertheless, further exploration of laser cutting of polymer materials is needed to increase cutting efficiency.

CO_2 laser cutting is useful in various industries and domestic applications because the demand for materials with low melting points, especially plastic polymers, continues to grow. Therefore, it remains a promising area of research for which a separate guidelines document is needed. Studies have shown that using a low-energy CO_2 laser can enhance cutting quality. These lasers are precise and capable of producing fine details. They can also cut PMMA with high edge quality and minimal heat-affected zone. [14]

This synthetic polymer is often used as an alternative to ordinary glass because of its properties, particularly its flexibility and optical properties. It is used in roofing, covering, fibbers optic production, telecommunications, and even the automotive and medical sectors. It is also suitable for outdoor use due to its high resistance to long-term exposure to ultraviolet radiation. It is produced by either block polymerization or extrusion. Both methods produce a transparent semi-finished product. In block polymerization, the final product is usually a plate or block. The advantage of this method is achieving a higher surface quality and better mechanical properties than with extrusion. However, extrusion production is cheaper and has better thickness tolerance. [15-17]

Previous studies have shown that laser cutting parameters, especially the focal length of the objective and the cutting speed, significantly impact the cutting width and surface quality, particularly when working with PMMA materials of different thicknesses. These parameters affect not only cutting accuracy but also the occurrence of thermal damage, such as melting or degradation of the material. This can lead to a change in the geometry of the cutting groove.

Based on these findings, this experiment focuses on a detailed comparison of the cross-sections of laser cuts made with different interpolated trajectories - specifically, circular and linear - using PMMA material. The goal is to evaluate how changes in trajectory affect cut quality, groove width, and the degree of thermal influence while maintaining the same working conditions as in the previous study. These results could contribute to optimizing cutting parameters for applications requiring high accuracy and minimal thermal influence on the material. [12]

2. Sample preparation for experiment

The samples were made using the ILS 3NM laser device, which is suitable for engraving PMMA, glass, rubber, textiles, plastic sheets, marble, and surface-treated metals. It can also cut the aforementioned materials, except glass, marble, and metals. When engraving, the maximum

cutting speed is 1524 mm/s, the maximum power is 100 W, and the following PPI settings are available: 166, 200, 250, 333, 500, and 1000.

For producing the samples, 3- and 5-mm-thick PMMA material was used. The samples were cut into 30-by-30-mm squares to compare the effect of the laser beam path on the cutting width. Lenses with focal lengths f of 38.1 mm (1.5" and 63.5 mm (2.5") were used. In a previous study, the gap was examined on a circular sample [12]. The working conditions used to cut the material through the entire thickness of the sample represented a maximum device power (P) of 100 watts. (100 percent) and a minimum cutting speed (v_f) of 45.72 mm/s, as well as a pulse per inch (PPI) of 1000, as shown in Table 1 for Figure 1.

Table 1. Working conditions for creating samples.

Sample groups	1	2	3	4
t (mm)	3	3	5	5
f (mm/")	38.1 / 1.5	63.5 / 2.5	38.1 / 1.5	63.5 / 2.5
v_f (mm·s^{-1})	45.72			
P (W/%)	100			

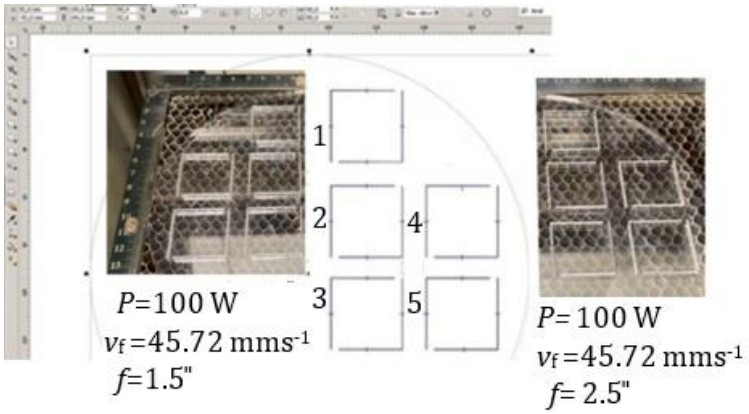

Figure 1. Sample preparation.

The testing of suitable cutting speeds was based on a previous study that focused on the effect of the laser beam on the width of a circular cut [12]. To compare the effects of cross-sectional trajectories (circle versus straight line), the working conditions were taken from the previous study. Using a 1.5" (38.1 mm) focal length lens, the 3 mm plate could be cut at all tested speeds. On the 5 mm board, cut-through occurred at a speed of 45.72 mm/s (which is 3 % of maximal speed), while lower speeds resulted in burning without cutting through the material. Similar behavior was exhibited by the 2.5" (63.5 mm) lens. Low speeds (15.24 mm/s and 30.48 mm/s) were not used for the 3 mm plate due to incomplete cuts. Higher speeds for the 5 mm plate were not applied because they led to material degradation. A 5 mm plate was only cut using a 4" (127.0 mm) lens at the lowest speed of 15.24 mm·s^{-1} (1 %). This cut resulted in significant surface melting, creating a wide cutting groove with rounded edges. [12]

3. Cutting width measurement

The measurement was taken with a Carl Zeiss workshop microscope (Figure 2) using a 10x magnification lens. This device allows for measurements with a resolution of 0.001 mm, and a measuring range of 200 mm longitudinally and 100 mmm transversely.

Measurements were performed on internal and external square samples made with lenses of 11.5" (38.1 mm) and 2.5" (63.5 mm) focal lengths on a 3-millimeter-thick plate with 100-watt power and a 45.72-millimeter-per-second cutting speed. Cutting along straight lines into the material was performed in unclosed square objects, which allowed for measurement of the internal and external dimensions of the square samples. All dimensions were measured on the upper and lower surfaces of the machined material in the vertical and horizontal directions (see Figure 3).

The interpretation and detailed description of the data in Figure 3 can be found in Section 4, "Results."

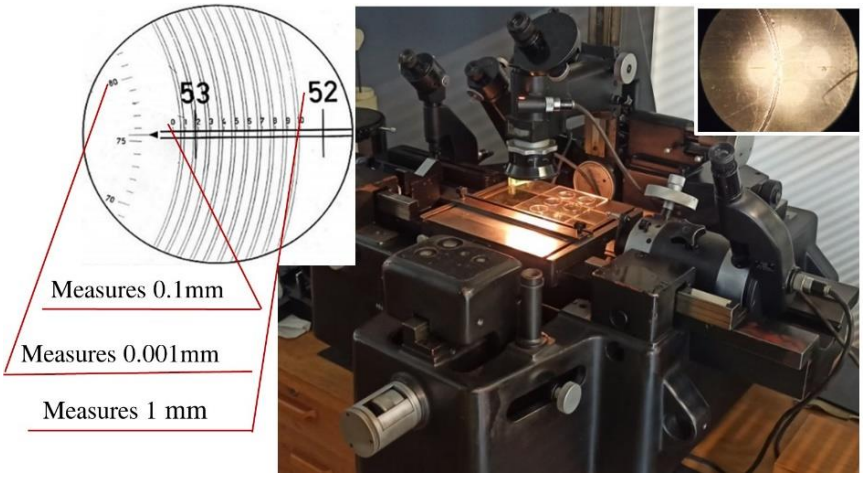

Figure 2. Measurement microscope Carl Zeiss.

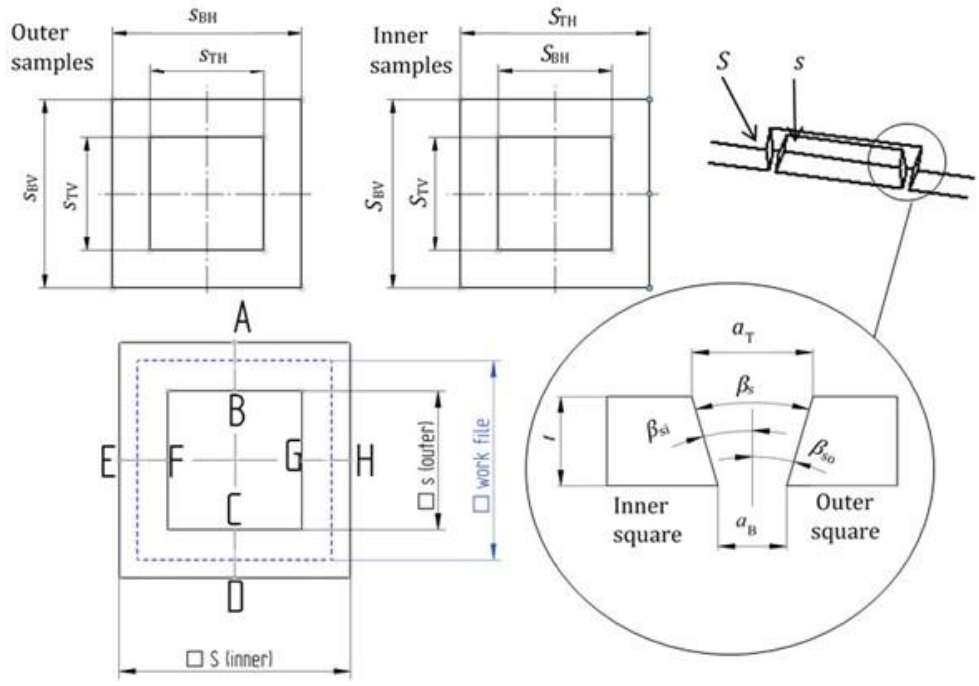

Figure 3. Scheme of measurement for determination width groove *a*, groove angle *ß* for square sample.

As an example, the data for sample group 3, a material with a thickness (t) of 5 millimetres and a focal length of 1.5 inches (38.1 millimetres), are shown in Table 2.

Table 2. Measured data for sample group 3.

Sample	1	2	3	4	5
Vertical direction (mm)					
A	0	0	0	0	0
B	0.394	0.285	0.271	0.384	0.355
C	29.959	29.911	29.971	29.957	29.939
D	30.245	30.213	30.291	30.226	30.296
B-A	0.394	0.285	0.271	0.384	0.355
D-C	0.386	0.302	0.320	0.269	0.357
[a]C-B	29.565	29.626	29.700	29.573	29.584
[b]D-A	30.245	30.213	30.291	30.226	30.296
[c](B-A)+(D-C)	0.680	0.587	0.591	0.653	0.712
Horizontal direction (mm)					
E	0	0	0	0	0
F	0.276	0.300	0.264	0.318	0.297
G	29.921	29.978	29.958	29.921	29.893
H	30.251	30.284	30.240	30.206	30.242
E-F	0.276	0.300	0.264	0.318	0.297
H-G	0.330	0.306	0.282	0.285	0.349
[d]G-F	29.645	29.678	29.694	29.603	29.596
[e]H-E	30.251	30.284	30.240	30.206	30.242
[f](F-E)+(H-G)	0.606	0.606	0.546	0.603	0.646

[a] S_{TV}, [b] S_{TV}, [c] $2a_{TV}$, [d] S_{TH}, [e] S_{TH}, [f] $2a_{TH}$.

4. Results

The evaluation focused on the dimensions of the samples, the width of the cutting grooves, and the chamfers formed by the laser beam as it travelled along a square path.

4.1 Dimensions of Squares

For each combination of parameters, the average of the measured values was calculated for the dimensions of the inner square on the top (S_T) and bottom (S_B) surfaces, the outer square on the top (s_T) and bottom (s_B) surfaces, and the groove on the top (a_T) and bottom (a_B) surfaces (Table 3, Figure 4).

The largest dimensions were achieved by applying a focal length of 2.5 inches (63.5 mm) to the upper surface of the sample. Differences in internal dimensions were less pronounced because the change in focal length did not significantly affect the volume of material removed by ablation. This effect was more evident in external dimensions. The greatest deviations were observed in samples with a sheet thickness of 3 millimeters. However, in most cases, the resulting values did not differ substantially from the external diameter measurements. The discrepancies observed can be attributed to the groove's predominant orientation towards the outer perimeter of the sample, which influenced material distribution.

Table 3. Dimensions of squares for different thicknesses and different focal lengths.

	" (mm)				" (mm)			
f	1.5 (38.1)				2.5 (63.5)			
	mm	mm	mm	mm	mm	mm	mm	mm
t	3	St.dev.	5	St.dev.	3	St.dev.	5	St.dev
s_{TV}	29.467	0.078	29.610	0.056	29.342	0.064	29.567	0.056
s_{BV}	29.506	0.037	29.685	0.040	29.513	0.056	29.712	0.064
s_{TH}	29.423	0.075	29.643	0.044	29.299	0.020	29.560	0.049
s_{BH}	29.521	0.066	29.738	0.021	29.568	0.062	29.900	0.171
S_{TV}	30.319	0.059	30.123	0.038	30.410	0.049	30.257	0.055
S_{BV}	30.390	0.124	30.294	0.045	30.338	0.046	30.069	0.097
S_{TH}	30.368	0.027	30.245	0.028	30.445	0.018	30.271	0.035
S_{BH}	30.283	0.643	30.133	0.022	30.232	0.069	30.257	0.213

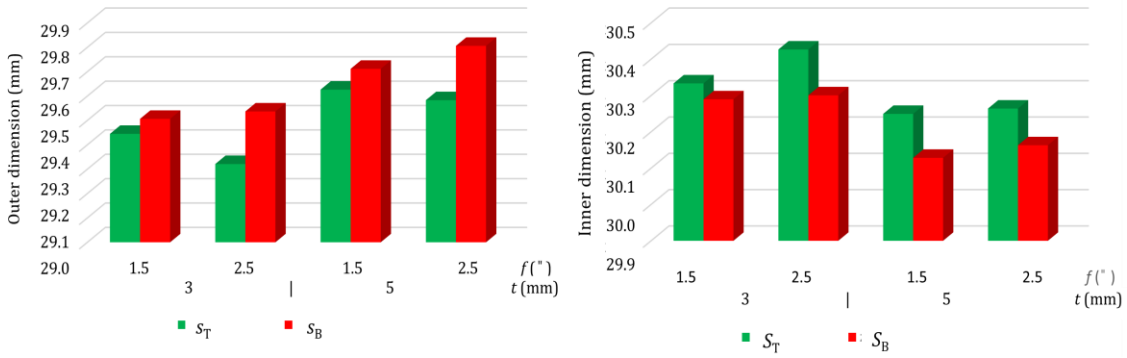

Figure 4. Dimension comparison for square samples.

4.2 Cutting width

Since the cross-section of the material varies depending on its thickness, it was expected that the geometry of the cut would vary over the depth of the materials [12].

The location and orientation of the grooves is defined by the designation of the width of the cut: a_{TV} is cutting width measured vertically on the top surface, a_{BV} is cutting width measured vertically on the bottom surface, a_{TH} is cutting width measured horizontally on the top surface, a_{BH} is cutting width measured horizontally on the bottom surface. The measured cutting widths are summarized in Table 4 and Figure 5.

Table 4. Cutting width for different thickness and focal lengths.

	" (mm)				" (mm)			
F	1.5 (38.1“)				2.5 (63.5“)			
	mm	mm	mm	mm	mm	mm	mm	mm
T	3	St. dev.	5	St. dev.	3	St. dev.	5	St. dev
a_{TV}	0.426	0.062	0.322	0.047	0,534	0.050	0.345	0.057
a_{BV}	0.392	0.034	0.219	0.023	0.412	0.069	0.179	0.044
a_{TH}	0.473	0.075	0.301	0.026	0.573	0.042	0,336	0.054
a_{BH}	0.381	0.046	0.198	0.130	0.342	0.046	0.178	0.040
a_{TV}- a_{BV}	0.034		0.103		0.122		0.166	
a_{TH}- a_{BH}	0.092		0.103		0.231		0.158	

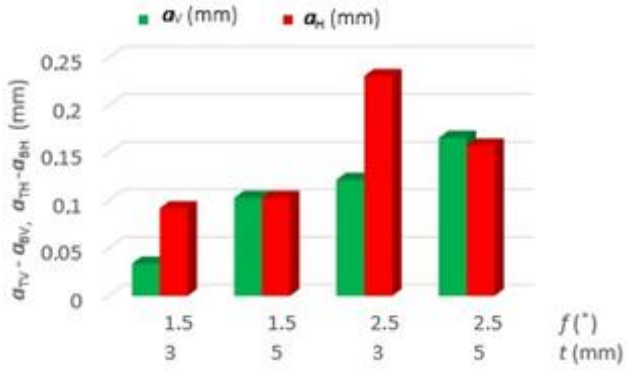

Figure 5. Dependence of widths on focal length and material thickness.

In all cases, the groove formed on the top surface of the material is wider than the groove formed on its bottom surface.For a material that is 3 millimeters thick, the difference in the width of the cut between the vertical and horizontal directions is more pronounced when using focal lengths of 1.5 inches (38.1 mm) and 2.5 inches (63.5 mm). For a material that is 5 millimeters thick, there is a slight difference in width between the horizontal and vertical directions when using the 1.5-inch focal length. A slight difference in groove width is also

achieved with a 5-millimeter-thick material when using the 2.5-inch focal length, but in this case, the groove width in the vertical direction was larger.

This difference is very small and could be caused by manufacturing inaccuracies. The size of the grooves is not symmetrically distributed along the cutting path. The graphics software defined this geometry as 30 millimeters. Table 5 shows the groove width in relation to the inner and outer squares. Therefore, the interface for the width distribution is the set sample geometry or the assumed laser beam trajectory.

Table 5. Areas of the width of the cut for square samples of 30 mm.

	" (mm)		" (mm)	
f	1.5 (38.1)		2.5 (63.5)	
	mm	mm	mm	mm
t	3	5	3	5
a_{TV}	0.426	0.345	0,534	0.345
s_{TV} / S_{TV} (%)	62.6 / 37.4	60.6 / 39.4	61.6 / 38.4	62.8 / 37.2
a_{BV}	0,322	0.179	0.413	0.179
s_{BV} / S_{BV} (%)	49.5 / 50.5	71.8 / 28.2	59.1 / 40.9	80.6 / 19.4
a_{TH}	0.472	0.336	0.573	0,336
s_{TH} / S_{TH} (%)	61.1 / 38.9	58.3 / 40.7	61.2 / 38.8	61.9/ 38.1
a_{BH}	0.291	0.178	0.342	0.1782
s_{BH} / S_{BH} (%)	62.8 / 37.2	66.2 / 33.8	65.1 / 34.9	27.9 / 72.1

Figure 3 and 6 show the achieved cutting widths relative to the defined path of the laser beam (dashed square). The displacement from the designed trajectory shows how the formed groove extends into the outer square *S* and the inner square *s*. The cuts' trajectory deviates significantly from the designed center. Positive values indicate an increase in the inner square, and negative values indicate an increase in the outer square.

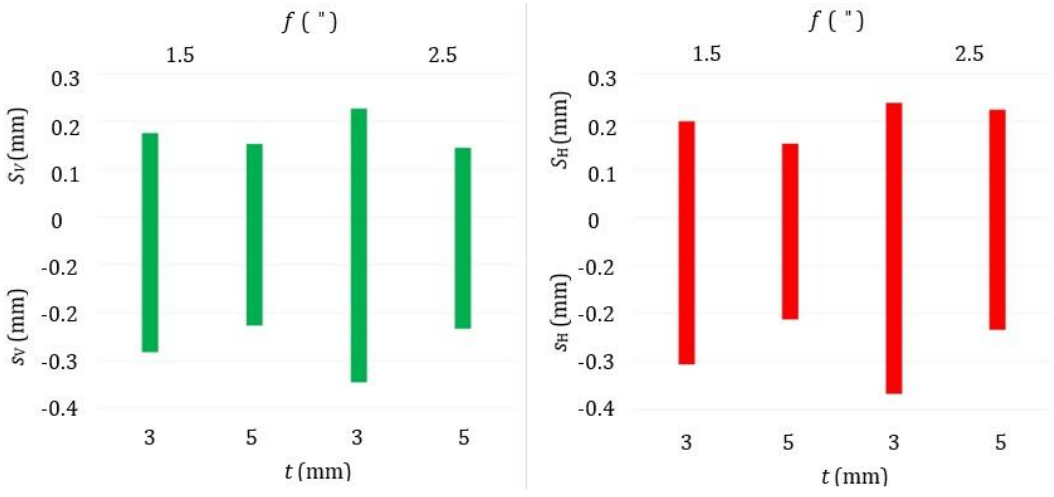

Measured in vertical direction Measured in horizontal direction

Figure 6. Groove width variance.

In the horizontal direction, the groove width was only slightly larger than that measured in the vertical direction. As the material thickness increased, deviations from the defined nominal dimension (30 mm) decreased slightly. This indicates the influence of the lenses used in the process.

4.3 Cutting chamfer

The groove widths in the horizontal direction were only slightly greater than those in the vertical direction, while the maximum angle of inclination occurred at a material thickness of 3 millimetres. For this material, the angles of α_{DV} (Table 6, Figure 3, 7) are considerably larger in the case of the inner diameter and the angles of α_{dV} of the outer diameter. This corresponds to the total angle α_V, which was formed by the cutting groove. A larger angle of chamfer on thinner material is caused to greater edge melting.

In the horizontal direction, the chamfer angles ($ß_H$)of the cuts were very similar to those observed angle ($ß_V$) in the vertical direction. The maximum chamfer angles were achieved when cutting 3 mm thick material using a focusing lens with a focal length of 2.5 inches. This effect may be attributed to the efficient beam penetration into the material, which facilitates melting of the cut surface and contributes to the formation of steeper chamfers.

Table 6. Chamfer of the cut for square 30 mm sample.

	" (mm)		" (mm)	
f	1.5 / 38.1		2.5 / 63.5	
	mm	mm	mm	mm
t	3	5	3	5
	(˚)	(˚)	(˚)	(˚)
$ß_{sv}$	5.079	2.394	6.257	2.481
$ß_{Sv}$	3.040	1.557	3.910	1.470
$ß_V$	8.119	3.951	10.168	3.951
$ß_{sH}$	5.491	2.243	6.667	2.382
$ß_{SH}$	3.502	1.567	4.238	1.466
$ß_H$	8.993	3.810	10.905	3.849

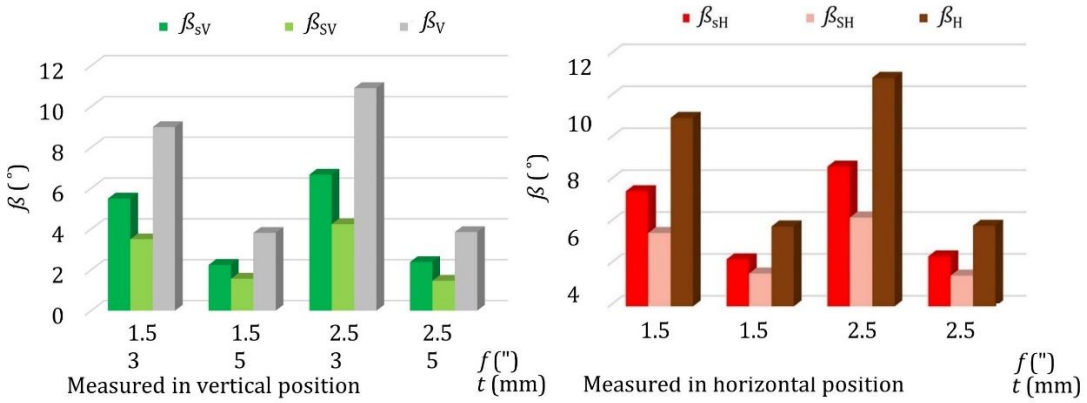

Figure 7. Comparison of cutting angle for square samples.

On the outer squares ($ß_{SV}$, $ß_{SH}$), the kerf taper (angle of the cut edge) was greater than on the inner squares ($ß_{SV}$, $ß_{SH}$), in both feed directions - horizontal and vertical. This suggests that beam divergence, cutting speed, and thermal load distribution may vary depending on the position within the cutting object.

4.4 Comparison of trajectories

To analyze the influence of the laser beam trajectory on cut quality, test objects in the shapes of circles and squares were used. These shapes allowed us to assess differences in inner and outer dimensions, kerf width, edge chamfer, and cutting angle. The objective was to determine how the laser's path - whether linear or circular - affects dimensional accuracy and edge quality.

The difference in dimensions when cutting along the circle's trajectory (d, D) and the line's trajectory (s, S) is evident. Larger values were achieved in all monitored parameters when cutting in straight lines (Figure 8).

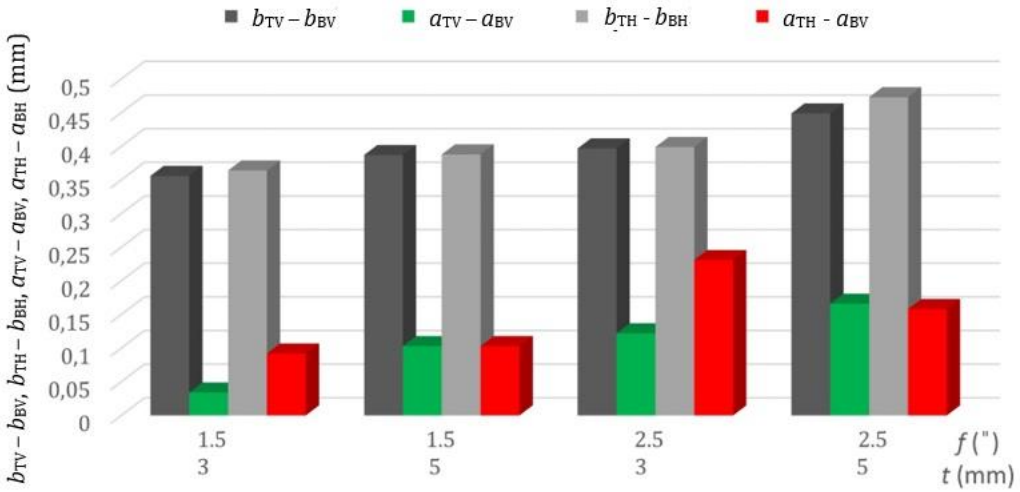

Figure 8. Comparison of cutting width in circular and linear trajectory.

The groove widths (a) produced by the square cut, specifically the differences $a_{TV} - a_{BV}$ and $a_{TH} - a_{BH}$, demonstrate greater variability depending on changes in focal length (f) and material thickness (t). The conditions are most pronounced at a focal length of 5 millimeters and a material thickness of 5 millimeters, which means that parameter a is sensitive to the optical process. Vertical differences ($a_{TV} - a_{BV}$) are generally higher than horizontal differences ($a_{TH} - a_{BH}$), suggesting that the vertical direction may influence cut width more than the horizontal direction.

On the other hand, the groove widths (b) created by cutting along the circle, i.e., the differences $b_T - b_{BV}$ and $b_{TH} - b_{BH}$, show smaller values and greater stability across all combinations of focal length and thickness [12]. In the horizontal direction, the differences (b_{TH}-b_{BH}) remain nearly constant, see Figure 8.

In the vertical direction, using a lens with a focal length (f) of 1.5 inches and a material thickness (t) of 3 millimetres, the cutting groove angle (α_V) generated along a circular trajectory was smaller than the groove angle (β_V) created along a linear trajectory. At a larger material thickness (t) of 5 millimetres, both angles decreased; however, in this case, the angle (α_V) resulting from the circular trajectory was larger than the angle produced by the linear path.

In this vertical direction, using a lens with a focal length (f) of 2.5 inches for a material with a thickness of 3 millimetres, the cutting angle formed by a circular trajectory (α_V) is larger than

the angle formed by a straight line (β_V). The effect of thickness on the cutting angle is a significant difference for the trajectory along a circle. The effect of thickness, using a focal length of 2.5 inches, was not observed for the trajectory.

In the horizontal direction, for a material with a thickness of 3 millimetres, the cutting angle was larger using a direct trajectory than a circular trajectory at both focal lengths. For a material with a thickness of 5 millimetres, the cutting angle was larger using a circular trajectory at the same focal lengths.

In the external shapes in the vertical direction (α_{dV}, β_{sV}), larger chamfer values were achieved for the straight trajectory, for both focal lengths and for both material thicknesses. For the external dimensions in the vertical direction (α_{DV}, β_{SV}), larger cutting-edge chamfers were achieved for the circular trajectory with a material thickness of 3 millimetres at a focal length setting of 2.5 inches, where there was a slight difference in the value of the larger chamfer when using the direct trajectory.

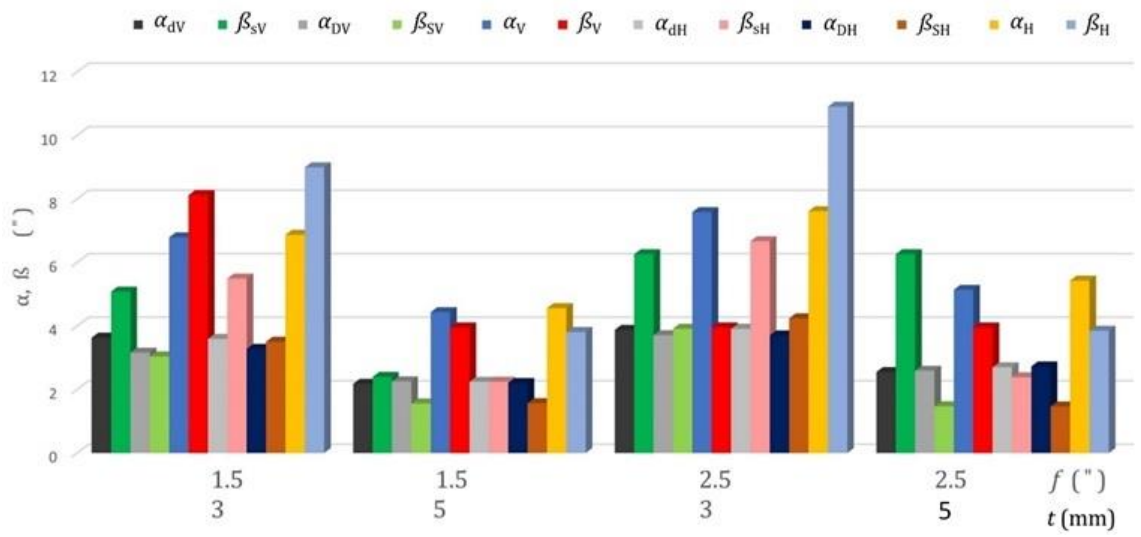

Figure 9. Comparison of angles.

In the horizontal direction, the internal shapes (α_{DH}, β_{SH}) produced larger chamfer in straight paths for the 3 millimetres material thickness using both focal lengths. For the 5 millimetres material, larger chamfer was produced along the circular trajectory, but of significantly smaller values, for both shapes, inner (D, S) and outer (d, s) than for the 3 millimetres material, as shown for Figure 9.

5. Conclusion

Experimental research has shown that the trajectory of the laser beam is critical to the quality and dimensional accuracy of PMMA CO_2 sheet metal cutting. While linear trajectories generally resulted in larger outer dimensions, smaller kerf widths, and more pronounced edge bevels - especially in the vertical direction - circular trajectories provided more stable results, smaller cutting angles, and, in many cases, higher dimensional regularity throughout the beam path. The influence of focal length and material thickness was also evident: thinner samples (3 mm) were more sensitive to beam divergence and heat accumulation, while thicker samples (5 mm) produced more consistent kerf widths and smaller bevel angles.

A key observation is that the kerf width on the top surface is consistently larger than on the bottom surface. This confirms the effects of beam convergence and thermal energy distribution throughout the material thickness. Additionally, the results suggest that a larger focal length (2.5“) tends to increase the bevel angle for thinner samples; however, this effect is less pronounced for thicker sheets. These findings underscore the importance of carefully selecting laser optics and process parameters according to material thickness and desired edge quality.

From a practical perspective, the study provides clear guidelines for optimizing laser cutting of PMMA, a material widely used in optics, telecommunications, automotive, and medical applications. Industries requiring high edge quality and precise dimensional tolerances can benefit from circular trajectories, especially when consistent geometry and smaller bevel angles are critical. Conversely, linear trajectories may be preferable when faster cutting and higher material removal are priorities, albeit at the expense of uniformity throughout the cutting path.

The presented results contribute to a deeper understanding of how laser beam interpolation strategies affect machining results. They also form the basis for the further integration of process optimization into digital manufacturing environments. In the context of Industry 4.0 and the emerging Industry 5.0 paradigm, in which artificial intelligence and adaptive process control are becoming increasingly important, experimentally validated datasets like this one are essential for developing predictive models and intelligent decision support systems. Future research should focus on expanding the material portfolio, exploring more complex geometries, and applying AI-based algorithms to optimize trajectory planning for sustainable, highly efficient laser manufacturing.

Acknowledgment

Acknowledgment goes to Mr. Michal Hanus for the measured data for evaluating the effects of the laser beam acting along the trajectory of the square.

References

[1] Ninikas K, Kechagias J. and Salonitis K 2021 The impact of process parameters on surface roughness and dimensional accuracy during CO_2 laser cutting of PMMA thin sheets. *J. Manuf. Mater. Process.* **5**(3) 74. https://doi.org/10.3390/jmmp5030074

[2] Petillon S, Knöller A, Bräuer P, Helm D, Grözinger T, Weser S, Eberhardt W, Franke J and Zimmermann A 2022 Flexural fatigue test - A proposed method to characterize the lifetime of conductor tracks on polymeric substrates. *J. Manuf. Mater. Process.* **6**(2) 41. https://doi.org/10.3390/jmmp6020041

[3] Zhou Z, Gao X and Zhang Y 2022 Research progress on characterization and regulation of forming quality in laser joining of metal and polymer, and development trends of lightweight automotive applications. *Metals* **12**(10) 1666. https://doi.org/10.3390/met12101666

[4] Deepika C, Taj K and Bedar P 2024 Automation in production systems: Enhancing efficiency and reducing costs in mechanical engineering. *Nanotechnol. Percept.* **20**(5) 1436. https://doi.org/10.62441/nano-ntp.vi.3895

[5] Murzin S P 2024 Artificial intelligence-driven innovations in laser processing of metallic materials. *Metals* **14** (12) 1458. https://doi.org/10.3390/met14121458

[6] Elhamali S, Musbah H, Zawi L, Shuwehdi A, Faris H and Mahdawe A 2025 Artificial intelligence meets laser technology: A review of recent advances. *Results Surf. Interfaces* **20** 100484. https://doi.org/10.1016/j.rsurfi.2025.100484

[7] Barari A, Tsuzuki M S G, Cohen Y and Macchi M 2021 Editorial: Intelligent manufacturing systems towards Industry 4.0 era. *J. Intell. Manuf.* **32** 1793–1796. https://doi.org/10.1007/s10845-021-01769-0

[8] Fernández-Miguel A, García-Muiña F E, Ortíz-Marcos S, Jiménez-Calzado M, Fernández del Hoyo A P and Settembre-Blundo D 2025 AI-driven transformations in manufacturing: Bridging Industry 4.0, 5.0, and 6.0 in sustainable value chains. *Future Internet* **17**(9) 430. https://doi.org/10.3390/fi17090430

[9] McDonnell M D T, Arnaldo D, Pelletier E, Grant-Jacob J A Praeger M, Karnakis D, Eason R W and Mills B 2021 Machine learning for multi-dimensional optimisation and predictive visualisation of laser machining. *J. Intell. Manuf.* **32** 1471–1483. https://doi.org/10.1007/s10845-020-01717-4

[10] Li C, Pan H, Bousseau A and Mitra N J 2020 Sketch2CAD: Sequential CAD modelling by sketching in context. *ACM Trans. Graph*. **39** (6) 164. https://doi.org/10.48550/arXiv.2009.04927

[11] Kubišová M, Pata V, Měřínská D, Škrobák A and Marcaník M 2021 Solving the issue of discriminant roughness of heterogeneous surfaces using elements of artificial intelligence. *Materials* **14** (10) 2620. https://doi.org/10.3390/ma14102620

[12] Knedlová J, Kubišová M, Pata V, Marcaník M and Bočáková B 2024 The effect of laser beam on the width of the cut. *J. Phys. Conf. Ser.* **2712** (1), 012019. https://doi.org/10.1088/1742-6596/2712/1/012019

[13] Okello J L, Fath El-Bab A M R, Yoshino M and El-Hofy H A 2024 Modelling of heat-affected zone (HAZ) in CO_2 laser micromachining of aluminium-coated polymethyl methacrylate (PMMA) using adaptive neuro-fuzzy inference system (ANFIS). *Multiscale Multidiscip. Model. Exp. Des.* **7** 617–629. https://doi.org/10.1007/s41939-023-00234-0

[14] Mushtaq R.T, Wang Y, Rehman M, Khan A M and Mia M 2020 State-of-the-art and trends in CO_2 laser cutting of polymeric materials—A review. *Materials* **13**(17) 3839. https://doi.org/10.3390/ma13173839

[15] Khoshaim A B, Elsheikh A H, Moustafa E B, Basha M and Showaib E A 2021 Experimental investigation on laser cutting of PMMA sheets: Effects of process factors on kerf characteristics. *J. Mater. Res. Technol.* **11** 112–125. https://doi.org/10.1016/j.jmrt.2021.01.012

[16] Zhang S, Xiong Z, Zhang J, Zhang X, Chen Y and Chen Y 2022 Mechanical properties and thermal analysis of graphene nanoplatelets reinforced polyimine composites. *e-Polymers* **22**(1) 696–704. https://doi.org/10.1515/epoly-2022-0060

[17] Edo G I, Ndudi W, Ali A B M, Yousif E, Zainulabdeen K, Onyibe P N, Akpoghelie P O, Ekokotu H A, Isoje E F, Igbuku U A, Essaghah A E A, Ahmed D S and Umar H 2024 An updated review on the modifications, recycling, polymerization, and applications of polymethyl methacrylate (PMMA). *J. Mater. Sci.* **59**, 20496–20539. https://doi.org/10.1007/s10853-024-10402-3